Inorganic Chemistry

ARTICLE

pubs.acs.org/IC

Synthesis and Characterization of a Series of Model Complexes of the Active Site of [Fe]-Hydrogenase (Hmd)

Dafa Chen,[†] Annegret Ahrens-Botzong,[‡] Volker Schünemann,[‡] Rosario Scopelliti,[†] and Xile Hu*[,†]

[†]Laboratory of Inorganic Synthesis and Catalysis, Institute of Chemical Sciences and Engineering, Ecole Polytechnique Fédérale de Lausanne (EPFL), SB-ISIC-LSCI, BCH 3305, Lausanne CH 1015, Switzerland

[‡]Fachbereich Physik, Technische Universität Kaiserslautern, D-67663 Kaiserslautern, Germany

Supporting Information

ABSTRACT: A series of Fe complexes were synthesized and characterized as small molecule mimics for the active site of [Fe]-hydrogenase (Hmd). The collection includes both structurally new compounds and analogues of previously reported models. These complexes contain the essential ligands of the enzyme, namely, acyl, CO, pyridone, and sulfur ligands. They serve as IR and Mössbauer spectroscopic models for the Fe center in [Fe]-hydrogenase. The field-dependent Mössbauer study of representative model complexes shows that the sign and absolute value of the quadrupole splitting are sensitive to the change in the ligand environment of the Fe center.

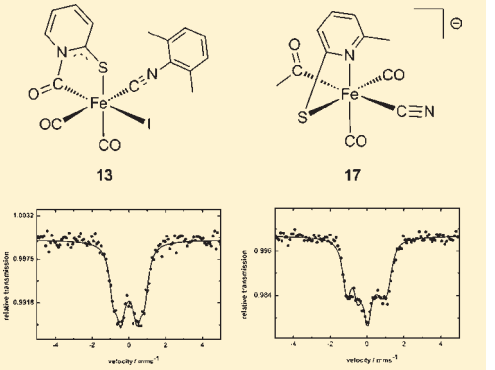

INTRODUCTION

Hydrogenases are enzymes that catalyze the production and utilization of hydrogen. Three classes of phylogenetically unrelated hydrogenases, namely, the [FeFe]-, [FeNi]-, and [Fe]-hydrogenases, are now known.[1−3] The [Fe]-hydrogenase, also termed as H_2-forming methylene-tetrahydromethanopterin dehydrogenase (Hmd), catalyzes the reduction of methenyl-tetrahydromethanopterin (methenyl-H_4MPT^+) with H_2 to form methylene-tetrahydromethanopterin (methylene-H_4MPT) and H^+ (Figure 1), an intermediary step in the reduction of CO_2 to methane by methanogens grown under nickel-limiting conditions.[4] Recent studies reveal several unique features of this enzyme. Unlike [FeFe]- and [FeNi] hydrogenases,[5−9] [Fe]-hydrogenase does not contain any Fe−S clusters and requires only one metal (Fe) for function.[2] The Fe center in [Fe]-hydrogenase, however, has a similar electronic structure (low-spin) and is ligated by similar ligands (sulfur and CO) as the distal Fe centers in [FeFe] and [FeNi]-hydrogenases.[2]

The composition and structure of the Fe-containing active site have been elucidated, albeit with some uncertainty, using a wide range of spectroscopic and crystallographic methods.[10−19] The current model suggests that the Fe ion is coordinated to two cis-CO ligands, a cysteine sulfur atom, a bidentate pyridone molecule through its nitrogen and acyl carbon atoms, and a yet unidentified ligand (Figure 2).[15] Because it is a recent discovery, only a few small molecule mimics of [Fe]-hydrogenase have been reported.[3,20−30] Such model compounds would be useful in studying the properties and catalytic activity of this interesting

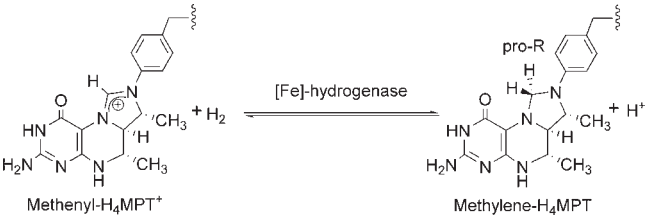

Figure 1. Hydride transfer reaction catalyzed by [Fe]-hydrogenase.

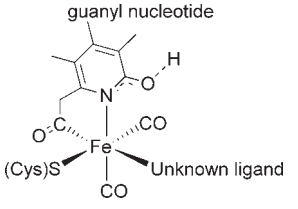

Figure 2. Proposed active site of [Fe]-hydrogenase.

enzyme. We recently communicated the synthesis of several structural mimics for the active site of [Fe]-hydrogenase, including those reproducing the first coordination sphere of [Fe]-hydrogenase.[27−29] Here we report the synthesis and reactivity of

Received: March 22, 2011
Published: May 03, 2011

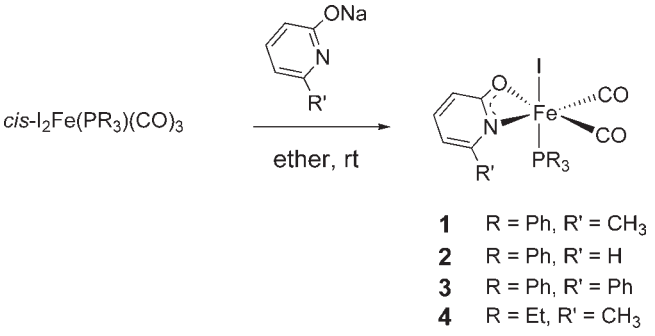

Figure 3. Synthesis of iron bis(carbonyl) pyridonate complexes.

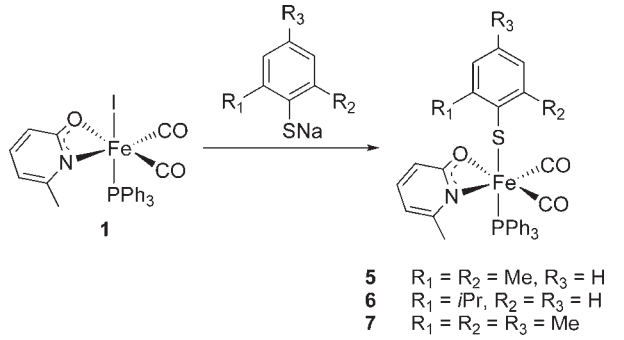

Figure 5. Synthesis of iron bis(carbonyl) pyridonate thiolate complexes.

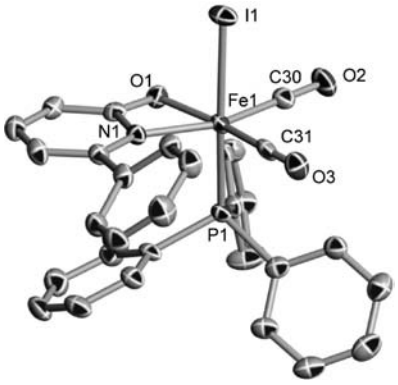

Figure 4. Solid-state structure of **3**. The thermal ellipsoids are displayed in 50% probability. Selected bond distances (Å) and angles (deg): Fe1−N1, 2.024(2); Fe1−O1, 1.996(2); Fe1−P1, 2.2828(8); Fe1−C30, 1.793(3); Fe1−C31, 1.796(3); Fe1−I1, 2.6691(5); C30−O2, 1.137(3); C31−O3, 1.133(4); C5−O1, 1.299(3); C5−N1, 1.357(4); C1−N1, 1.357(4); C30−Fe1−C31, 91.93(13); O1−Fe1−N1, 66.08(9). A phenyl group in the PPh_3 is disordered and modeled over two sites. For clarity, only one site is shown.

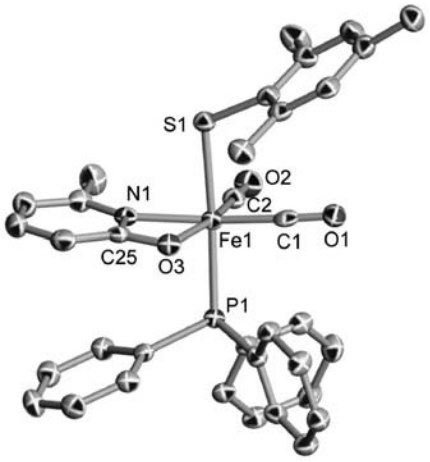

Figure 6. Solid-state molecular structure of complex **7**. The thermal ellipsoids are displayed at 50% probability. Selected bond distances (Å) and angles (deg): Fe1−N1, 1.998(3); Fe1−O3, 2.047(3); Fe1−P1, 2.2778(11); Fe1−C1, 1.788(4); Fe1−C2, 1.773(4); Fe1−S1, 2.3444(11); C1−O1, 1.143(5); C2−O2, 1.143(5); C25−O3, 1.312(5); C25−N1, 1.354(5); C1−Fe1−C2, 89.35(18); O3−Fe1−N1, 65.80(12).

some additional Fe model complexes, as well as Mössbauer studies on representative structural models.

RESULTS AND DISCUSSION

1. Synthesis and Reactivity of Iron Pyridonate Complexes. *1.1. Synthesis and Structure of Iron Pyridonate Iodide Complexes.* We initially used simple pyridonate ligands to mimic the pyridone cofactor found in [Fe]-hydrogenase. We showed earlier that reaction of $Fe(CO)_3(PPh_3)I_2$ with sodium 6-methyl-2-pyridonate (PyO_1) yielded $Fe(CO)_2(PPh_3)I(PyO_1)$ (**1**).[27] Analogous reactions produced several other iron bis(carbonyl) pyridonate derivatives **2**−**4** (Figure 3). Complexes **2**−**4** are characterized by IR, NMR, elemental analysis, and X-ray crystallography.[31] The two CO ligands are mutually cis, and the pyridonate ligand binds Fe in a η^2-κ-N,O fashion in all complexes. The Fe-PyO fragment is best described by a mixture of two resonance forms, in which PyO exists in either deprotonated pyridinol or deprotonated pyridone form. All Fe-ligand and C−O bond distances are comparable in complexes **1**−**4**. A structural drawing of **3** is shown in Figure 4; those of **2** and **4** can be found in the Supporting Information.

1.2. Synthesis and Structure of Iron Pyridonate Thiolate Complexes. With Fe pyridonate iodide complexes in hand, we

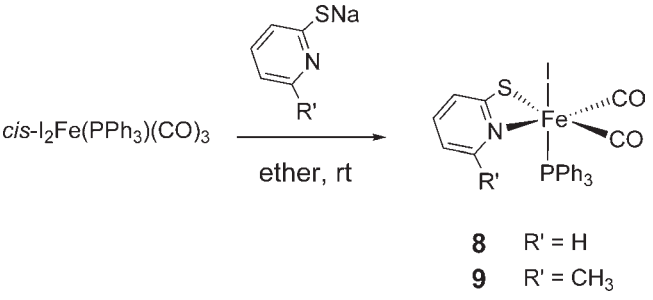

Figure 7. Synthesis of iron bis(carbonyl) pyridyl-2-thiolate complexes.

sought to install sulfur ligands to mimic the cysteine ligand of [Fe]-hydrogenase. Complex **1** reacted with sodium aryl thiolate to give $Fe(CO)_2(PPh_3)(PyO_1)SAr$ (Ar = 2,6-$Me_2C_6H_3$ (**5**), 2-*i*PrC_6H_4 (**6**), 2,4,6-$Me_3C_6H_2$ (**7**), Figure 5). The synthesis of **5** was briefly communicated, but no single crystals could be obtained, precluding its structural confirmation.[27] Single crystals suitable for X-ray diffraction study, however, can be obtained for complexes **6** and **7**. No stable species could be isolated from the reactions of **2**−**4** with ArSNa (Ar = 2,6-$Me_2C_6H_3$, 2-*i*PrC_6H_4, 2,4,6-$Me_3C_6H_2$).

dx.doi.org/10.1021/ic200580z |*Inorg. Chem.* 2011, 50, 5249–5257

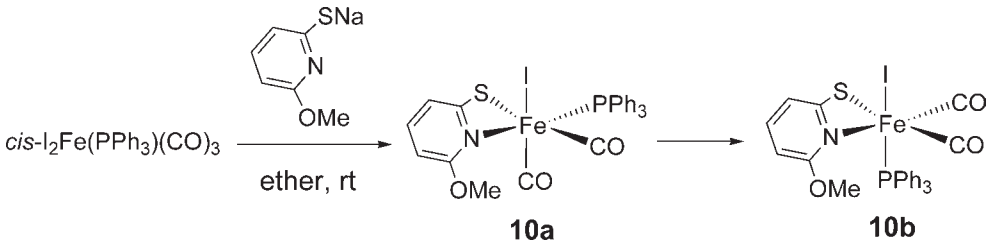

Figure 8. Synthesis of complexes **10a** and its isomerization to **10b**.

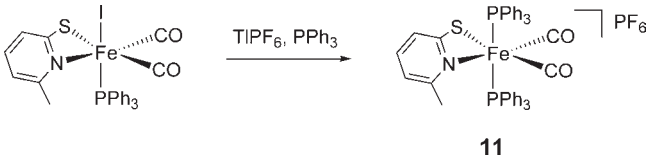

Figure 9. Synthesis of iron complex **11**.

Complexes **6** and **7** exhibit the same "$Fe(CO)_2(PR_3)(PyO)$" core with similar bond lengths and angles as complexes **1**−**4**. There is insignificant change in the CO bond distances upon substitution of I with SAr, even though IR data suggest a higher degree of metal-to-ligand π-backbonding in **6** and **7** (see below). The thiolate ligands coordinate to only one Fe center in spite of their tendency to form bridging dimers with Fe carbonyl complexes. A structural drawing of **7** is shown in Figure 6; that of **6** can be found in the Supporting Information.

We found that a phosphine ligand is essential for the isolation and stability of model complexes **1**−**7**. Attempts to substitute the phosphine ligand by another N donor ligand were unsuccessful.

Complexes **1**, **6**, and **7** do not react with H_2 nor with CO. Complexes **6** and **7** decompose rapidly (in hours) in solution at room temperature.

2. Synthesis and Reactivity of Iron Complexes Containing Pyridyl-2-thiolate Ligands. Parallel to the work with pyridone ligands, we also employed pyridyl-2-thiolate ligands to mimic the N,S ligands found in the active site of [Fe]-hydrogenase. Reaction of $Fe(CO)_3(PPh_3)I_2$ with sodium 6-R′-pyridyl-2-thiolate (R′ = Me, H) yielded $Fe(CO)_2(PPh_3)I$(R′-PyS) (**8** and **9**, Figure 7). In both complexes, the I^- and PPh_3 ligands are mutually trans. The synthesis and structure of compound **8** were recently reported by Darensbourg et al.[23]

When monitoring the reaction of $Fe(CO)_3(PPh_3)I_2$ with sodium 6-Me-pyridyl-2-thiolate by ^{31}P NMR, we found that besides the signal at 73.2 ppm which belongs to **9**, there was another weak peak at 52.3 ppm. Attempts to isolate this minor species were unsuccessful. However, in the analogous reaction of 6-OMe-pyridyl-2-thiolate with $Fe(CO)_3(PPh_3)I_2$ (Figure 8), after 0.5 h in ether, *cis*-(I, PPh_3)-$Fe(CO)_2(PPh_3)$I(OMe-PyS) (**10a**) was isolated as the product. The ^{31}P NMR spectrum of **10a** shows one signal at 51.1 ppm. **10a** isomerizes to *trans*-(I, PPh_3)-$Fe(CO)_2(PPh_3)$I(OMe-PyS) (**10b**) quantitatively in solution overnight. The X-ray structures of **10a** and **10b** are shown in the Supporting Information. The ^{31}P NMR spectrum of **10b** shows only one signal at 75.3 ppm, comparable to the ^{31}P signal of **8** and **9**. On the basis of these observations, the minor species observed in the synthesis of **9** should be its isomer, *cis*-(I, PPh_3)-$Fe(CO)_2$-(PPh_3)I(Me-PyS). It appears that in all these complexes, the trans-isomers are thermodynamically more stable.

Despite many attempts, we were not able to replace the I anion in **8** and **9** with another anionic ligand. Abstraction of I^- by Ag or Tl cation did not lead to a stable compound. Reaction of **9** with $TlPF_6$ in the presence of PPh_3 gave the bis(phosphine) complex **11** (Figure 9). The structure of **11** was confirmed by X-ray crystallography.[31]

Interestingly, a different reactivity was observed with the isocyanide substituted precursor $Fe(CO)_3$(2,6-dimethyl-PhNC)I_2 (**12**). Reaction of **12** with sodium pyridyl-2-thiolate gave complex **13** (Figure 10). The structure of **13** is shown in Figure 11. The Fe ion is coordinated to two cis-carbonyls, one iodide anion, the isocyanide ligand, and an unexpected acyl, thiolate chelate. The latter ligand could be considered as the product of CO migration into the pyridyl-2-thiolate ligand. Presumably, the reaction first yielded the substitution product **13*** and one molecule of CO, which then inserted into the nucleophilic Fe−N bond to give the **13** (Figure 10). Consistent with this hypothesis, the yield of **13** was higher when the reaction was carried out in the presence of CO.

3. IR Spectra of Model Complexes. Complexes **1**−**11**, **13** all display two strong IR absorption bands between 2050 and 1950 cm^{-1}, arising from the two terminal CO ligands (Table 1). The intensities of the two bands are similar, indicating that the two CO ligands bind in a cis-fashion, with a CO−Fe−CO angle of near 90 °C. This result is consistent with the crystal structures of the complexes. The averaged CO vibration frequencies of all Fe^{II} model complexes are within the range found for monomeric Fe^{II} bis(carbonyl) complexes.[21,23] Substitution of PPh_3 by PEt_3 increases the electron density at the Fe center, and lowers the averaged CO stretching frequency for about 10 cm^{-1} (**1** vs **4**). The substituent at the 6-position of the pyridone ligand has a small but noticeable effect in the CO stretching frequencies (compare **1**−**3**). Substitution of I by SAr also makes the Fe center more electron rich and lowers CO stretching frequencies for about 10 cm^{-1} (**1** vs **6** and **7**). The pyridyl-2-thiolate ligand is slightly more electron rich than the pyridonate ligand (**1** vs **9**, and **2** vs **8**), lowering the IR frequency of about 10 cm^{-1}. As expected, the ν_{CO} in the cationic complex **11** is much higher than in the neutral complex **9**. Compared to [Fe]-hydrogenase and our previously reported Fe acyl complexes (e.g., **15**−**17**, Figure 12),[28] the Fe centers in the current model complexes are slightly less electron rich.

4. Mössbauer Studies of Representative Model Complexes. One of the most useful tools to study the electronic structure of Fe compounds is ^{57}Fe Mössbauer spectroscopy.[32−34] Field-dependent Mössbauer studies of [Fe]-hydrogenase found an isomeric shift of $\delta = +0.06$ mm s^{-1} and a positive quadrupole splitting ($\Delta E_Q = +0.65$ mm s^{-1}) for the diamagnetic Fe center.[12] Very few Mössbauer studies have been conducted on model complexes,[21,23,27] and we earlier reported so far the only

dx.doi.org/10.1021/ic200580z |*Inorg. Chem.* 2011, 50, 5249–5257

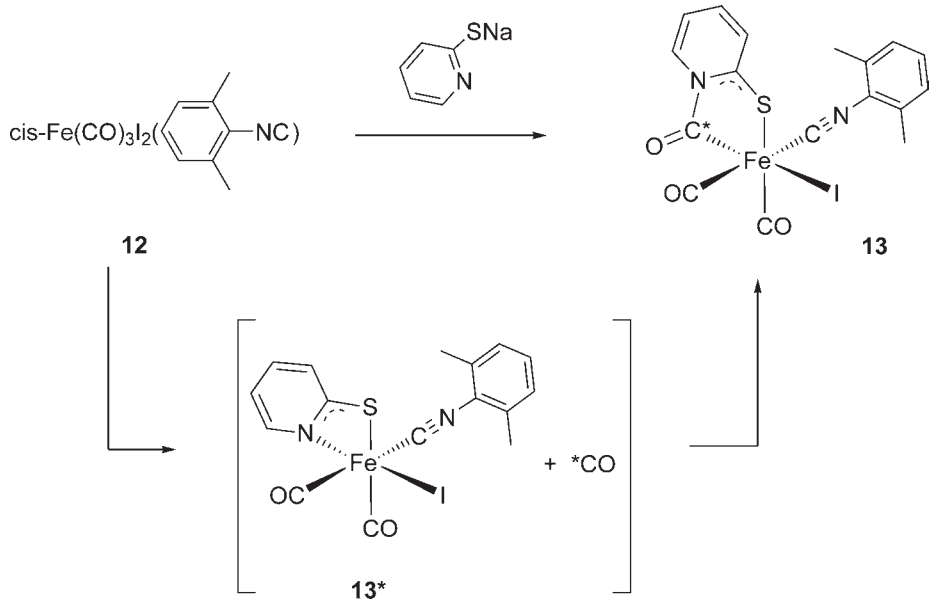

Figure 10. Synthesis of iron complex **13**.

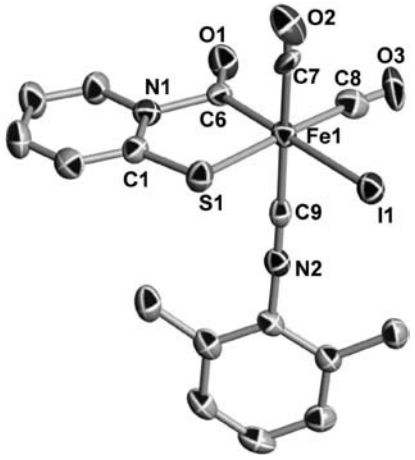

Figure 11. Solid-state molecular structure of complex **13**. The thermal ellipsoids are displayed at 50% probability. Selected bond distances (Å) and angles (deg): Fe1−C6, 1.941(5); Fe1−C7, 1.891(8); Fe1−C8, 1.827(7); Fe1−C9, 1.879(6); Fe1−S1, 2.2940(17); Fe1−I2, 2.6461(9); C6−O1, 1.144(7); C7−O2, 0.989(8); C8−O3, 1.059(8); C9−N2, 1.155(7).

Table 1. Selected Infrared Data

complex	ν_{CO} (cm^{-1})	complex	ν_{CO} (cm^{-1})
1[a]	2032, 1987	**10b**	2024, 1977
2	2039, 1988	**11**	2050, 1989
3	2035, 2001	**13**	2041, 2007
4	2026, 1974	**15**[b]	2016, 1968
5[a]	2021, 1967	**16**[b]	2003, 1931
6	2025, 1985	**17**[b]	1998, 1932
7	2021, 1973	Hmd[c]	2011, 1944
8	2028, 1986	Hmd + CO[c]	2020, 1981
9	2018, 1968	Hmd + KCN[c]	2020, 1956
10a	2031, 1980	Hmd cofactor[c]	2031, 1972

[a] Data from ref 27. [b] Data from ref 28. [c] data from ref 11.

field-dependent Mössbauer study of a model complex, **1**.[27] Field-dependent study is required to determine the sign of the quadrupole splitting and to confirm the diamagnetic ground state of the Fe center. Through the current and earlier synthetic efforts, we have access to a large number of Fe model complexes. This prompts us to carry out a comprehensive Mössabuer study on representative model complexes. These complexes are shown in Figure 12.

Two measurements were taken for each of the 8 complexes (**5**, **7**, **9**, **13**, **14**−**17**). One is taken at 55 K, 77 or 100 K in the absence of an external field, and one is taken at 5 K with an external field of 5 T perpendicular to the γ-ray. All samples show one component, except the sample for **17** which shows two components of 94% and 6% abundance at zero field and 77 K (Supporting Information, Figure S10). The major component corresponds to complex **17** while the minor component is attributed to a high-spin Fe^{II} impurity ($S = 2$). This minor component is not observable under a magnetic field, probably because of detection limits. The diamagnetic ground state is found for all complexes. Table 2 lists the Mössbauer parameters of these 8 complexes as well as those of **1**. Figures 13−16 show the Mössbauer spectra of complexes **7**, **14**, **15**, and **16**. The spectra of the other complexes can be found in the Supporting Information.

The isomeric shifts (δ) for all Fe model complexes shown in Figure 12 fall into a small range between 0.10 and −0.02 mm s^{-1}. The δ-values of model complexes are comparable to those found for [Fe]-hydrogenase[12] and its CO and CN-inhibited forms, and those of other Fe^{II} model complexes.[21,23] Thus, the low-spin Fe bis(carbonyl) core in these complexes has a major influence on their isomeric shifts. Nevertheless, examination of the δ-values of this series of related complexes reveals the smaller but observable influence of other ligands. Substitution of I with thiolate ligands resulted in a small decrease in the isomeric shifts (compare **1** with **5** and **7**, Table 2). Substitution of I with acyl ligand resulted in an even larger reduction in the isomeric shift (compare **9** and **16**,

dx.doi.org/10.1021/ic200580z |*Inorg. Chem.* 2011, 50, 5249–5257

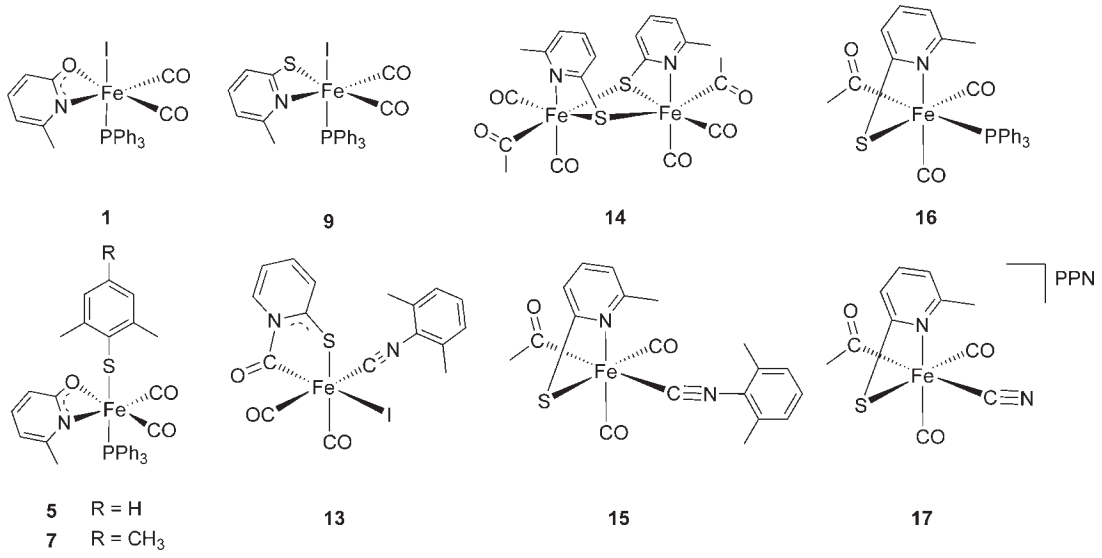

Figure 12. Fe model complexes for the Mössbauer study; PPN = bis(triphenylphosphine)iminium.

Table 2. Mössbauer Parameters for Model Complexes and [Fe]-Hydrogenase

complex	T/K	B/T	rel. contribution %	δ/mms^{-1}	ΔE_Q/mms^{-1}	Γ/mms^{-1}	η
1[a]	55		100	0.10 (±0.02)	(+) 0.48 (±0.02)	0.57 (±0.03)	
	5	5	100	0.10 (±0.02)	(+) 0.48 (±0.02)	0.40 (±0.03)	0
5	100		100	0.06 (±0.02)	(−) 0.83 (±0.02)	0.58 (±0.02)	
	5	5	100	0.04 (±0.02)	−0.87 (±0.03)	0.44 (±0.02)	0.6 (±0.2)
7	100		100	0.04 (±0.02)	(−) 0.84 (±0.05)	0.49 (±0.02)	
	5	5	100	0.06 (±0.02)	−0.89 (±0.02)	0.42 (±0.02)	0.2 (±0.2)
9	77		100	0.10 (±0.01)	(−) 0.35 (±0.03)	0.45 (±0.05)	
	5	5	100	0.11 (±0.02)	−0.36 (±0.03)	0.40 (±0.02)	0 (±0.5)
13	77		100	0.01 (±0.02)	(+) 0.29 (±0.02)	0.45 (±0.05)	
	5	5	100	0.01 (±0.02)	+0.29 (±0.04)	0.47 (±0.03)	0.6 (±0.4)
14	77		100	0.06 (±0.01)	(−) 0.74 (±0.02)	0.38 (±0.02)	
	5	5	100	0.06 (±0.02)	−0.67 (±0.02)	0.44 (±0.02)	0.4 (±0.1)
15	100		100	0 (±0.02)	(+) 0.73 (±0.02)	0.36 (±0.02)	
	5	5	100	0.01 (±0.01)	+0.72 (±0.02)	0.43 (±0.02)	0.5 (±0.1)
16	77		100	0 (±0.02)	(−) 1.14 (±0.02)	0.36 (±0.02)	
	5	5	100	0 (±0.02)	−1.14 (±0.04)	0.40 (±0.02)	0.4 (±0.1)
17	77		94	−0.02 (±0.02)	(+) 0.89 (±0.02)	0.57 (±0.02)	
			6	0.98 (±0.02)	3.16 (±0.02)	0.35 (±0.02)	
	5	5	100	−0.01 (±0.02)	+0.91 (±0.03)	0.47 (±0.02)	0.1 (±0.1)
Hmd (pH = 8.0)[b]	80		100	0.06	+0.65	0.32	
	4.2	4	100	0.06	+0.65	0.32	0.3 (±0.2)
Hmd + CO[b]	80		99	−0.03	−1.38	0.29	
	4.2	4	99	−0.03	−1.38	0.29	0.5 (±0.1)
Hmd + KCN[b]	80		100	−0.001	−1.75	0.38	
	4.2	4	100	−0.001	−1.75	0.38	0.6 (±0.1)
extracted Hmd cofactor (pH = 6.0)[b]	80		84	0.03	0.43	0.31	

[a] Data from ref 27. [b] Data from ref 12.

Table 2). The presence of π-acceptor ligands (CN^-, and RNC) reduces the isomeric shifts, so complexes **13**, **15**, and **17** have δ-values at the low end. This is consistent with the results from the Mössbauer studies of the enzymes which showed that binding of external CO or CN^- lowered the isomeric shifts of the Fe ion.[12] Interestingly, PPh_3 ligand appears to have a similar influence as CN^- and RCN (compare **16** with **15** and **17**, Table 2).

The small change in the isomeric shifts of the model complexes can be rationalized considering the electronic structure of these complexes. Isomeric shifts depend on the electron density

dx.doi.org/10.1021/ic200580z |*Inorg. Chem.* 2011, 50, 5249–5257

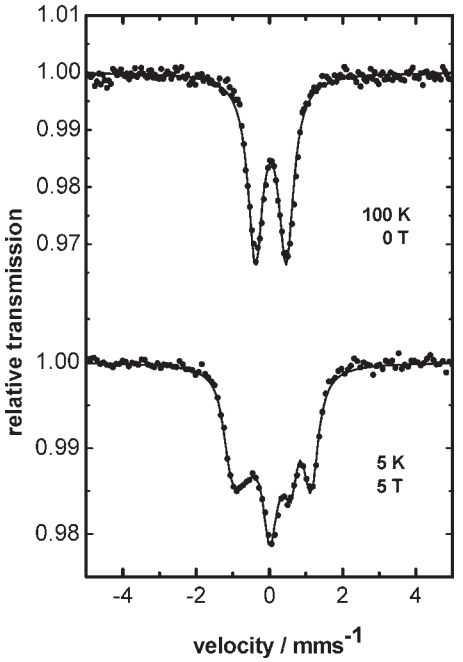

Figure 13. (Top) Mössbauer spectrum of **7** obtained at $T = 100$ K. The solid line represents a fit assuming Lorentzian line shape with parameters given in Table 2. (Bottom) Mössbauer spectrum of **7** obtained at 5 K and 5 T. The solid line represents a simulation assuming a diamagnetic ground state, with the parameters given in Table 2.

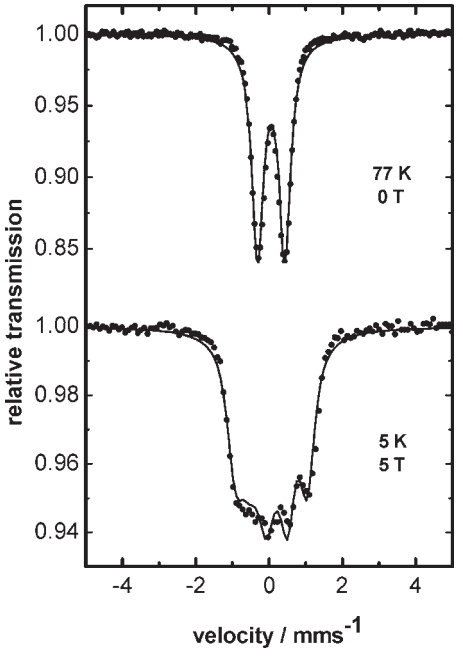

Figure 14. (Top) Mössbauer spectrum of **14** obtained at $T = 77$ K. The solid line represents a fit assuming Lorentzian line shape with parameters given in Table 2. (Bottom) Mössbauer spectrum of **14** obtained at 5 K and 5 T. The solid line represents a simulation assuming a diamagnetic ground state, with the parameters given in Table 2.

at the nucleus, and almost exclusively the s electrons.[32,34] For Fe compounds, a higher s electron density at the nucleus results in a lower (more negative) isomeric shift. The outer s electrons are shielded by the valence d electrons. The 8 model complexes are

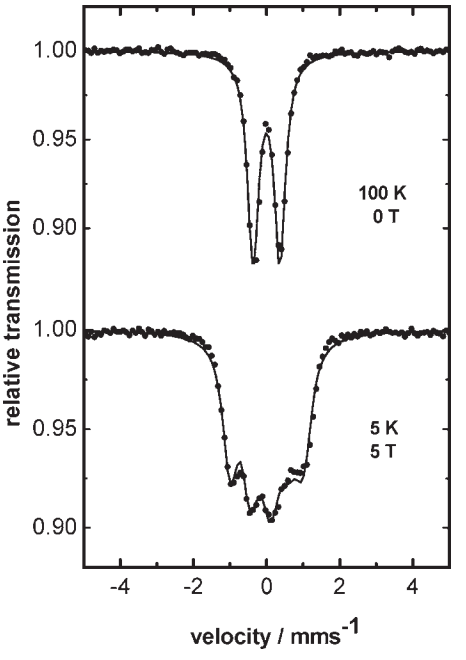

Figure 15. (Top) Mössbauer spectrum of **15** obtained at $T = 100$ K. The solid line represents a fit assuming Lorentzian line shape with parameters given in Table 2. (Bottom) Mössbauer spectrum of **15** obtained at 5 K and 5 T. The solid line represents a simulation assuming a diamagnetic ground state, with the parameters given in Table 2.

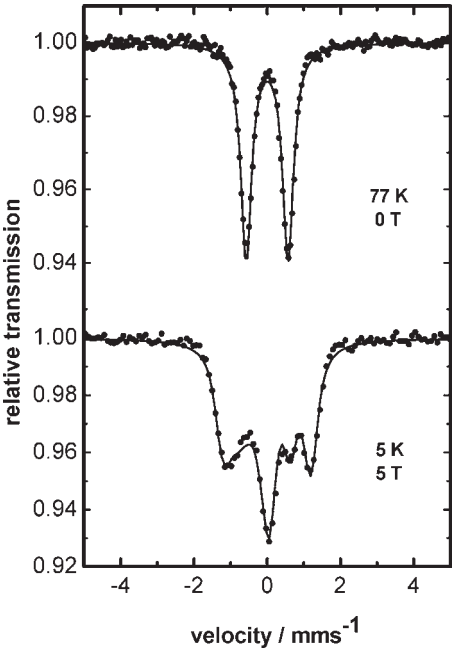

Figure 16. (Top) Mössbauer spectrum of **16** obtained at $T = 77$ K. The solid line represents a fit assuming Lorentzian line shape with parameters given in Table 2. (Bottom) Mössbauer spectrum of **16** obtained at 5 K and 5 T. The solid line represents a simulation assuming a diamagnetic ground state, with the parameters given in Table 2.

all low spin Fe(II), so they have the same electronic configurations. Therefore, their isomeric shifts are similar. When the π-donor ligand iodide in a complex is replaced by thiolate or

dx.doi.org/10.1021/ic200580z |*Inorg. Chem.* 2011, 50, 5249–5257

acyl ligands, or when the complexes contain π-acceptor ligands, there is a small decrease in the d electron density at the metal center. Consequently, the shielding of the outer s electrons decreases, and hence the isomeric shifts slightly decrease.

There is no clear correlation between the IR and Mössbauer parameters (Supporting Information, Figure S11). In some cases, lower isomeric shifts are found for compounds having lower ν_{CO} (compare **1** with **5** and **7**, Tables 1 and 2). In other cases, different isomeric shifts are found for compounds having very similar ν_{CO} (compare **7** with **9**). There are also cases where similar isomeric shifts are found for compounds having different ν_{CO} (compare **15** with **16**, and **13** with **15**). Finally, there are cases when lower isomeric shifts are found for compounds having higher ν_{CO} (compare **9** with **13**). The discrepancy between IR and Mössbauer parameters reflects the different origin of these spectroscopic data. The ν_{CO} is an indication of the Fe-to-CO π-backbonding, whereas the isomeric shift is an indication of the s electron density at the ^{57}Fe nucleus.

The quadrupole splitting ΔE_Q varies significantly. Complexes containing iodide ligands (**1**, **9**, and **13**) have lower absolute ΔE_Q values (ca. 0.3 to 0.5 mms^{-1}); the other complexes have absolute ΔE_Q values between 0.7 and 1.1 mms^{-1}. According to Table 2, substitution of one ligand on a given complex results in a sustainable change in the absolute values of ΔE_Q and sometime even the sign of the quadrupole splitting. For example, substitution of I^- with a thiolate ligand (from **1** to **5** and **7**) changes ΔE_Q from +0.48 to about −0.85 mms^{-1}. Likewise, substitution of the isocyanide ligand in **15** with PPh_3 (in **16**) changes ΔE_Q from +0.72 to −1.14 mms^{-1}; further substitution with CN^- (in **17**) then changes ΔE_Q to +0.91 mms^{-1}. Similar changes in ΔE_Q were observed for [Fe]-hydrogenase: treatment of Hmd with CO or KCN resulted in a change of ΔE_Q from +0.65 to −1.38 and −1.75 mms^{-1}, respectively.[12]

The change in the quadrupole splitting is attributed to the change of ligand environment. The quadrupole splitting arises from the interaction between the electric field gradient (EFG) and the nuclear quadrupole moment.[32,34] It is a sensitive probe for the chemical environment of the Fe center which determines the EFG. The total EFG can be separated into two contributions. In a noncubic symmetry, the charges on ligands surrounding the Fe atom give rise to the lattice contribution. On the other hand, the noncubic distribution of electrons in partially filled valence orbitals of the Fe ion generates the valence contribution. The model complexes measured here are all low-spin d,[6] and all t_{2g} orbitals are filled. The valence contributions vanish. The lattice contributions, however, are very different when the ligands are different. Changing one ligand will perturb the magnitude and sign of the lattice contribution. Therefore, very different quadrupole splitting parameters were detected among the model complexes, as well as different states of the enzymes.

CONCLUSION

In summary, a series of Fe model complexes for the active site of [Fe]-hydrogenase are synthesized and structurally characterized. Some of them are analogues to previously reported models (complexes **2**−**4**, **8**, **9**); others are structurally new compounds (complexes **6**, **7**, **10**, **13**). These complexes serve as IR and Mössbauer spectroscopic models for the Fe center in [Fe]-hydrogenase. The averaged CO vibration frequencies and the isomeric shifts of the model complexes fall into a narrow range, and are comparable to the values determined for the enzymes. The field-dependent Mössbauer study of the model complexes shows that the sign and absolute value of the quadrupole splitting is very sensitive to the change in the ligand environment of Fe centers.

EXPERIMENTAL SECTION

A. Chemicals and Reagents. All manipulations were carried out under an inert N_2(g) atmosphere using glovebox techniques. Solvents were purified using a two-column solid-state purification system (Innovative Technology, NJ, U.S.A.) and transferred to the glovebox without exposure to air. Deuterated solvents were purchased from Cambridge Isotope Laboratories, Inc., and were degassed and stored over activated 3 Å molecular sieves. All other reagents were purchased from commercial sources. Liquid compounds were degassed by standard freeze−pump−thaw procedures prior to use. Complexes $Fe(CO)_3(PPh_3)I_2$, $Fe(CO)_3(PEt_3)I_2$, $Fe(CO)_3I_2$(2,6-$Me_2C_6H_3NC$), [$Fe(CO)_2(PPh_3)$I(hmp)] (**1**), and [$Fe(CO)_2(PPh_3)$(hmp){S(2,6-$Me_2C_6H_3$)}] (**5**) (Hhmp = 2-Hydroxy-6-methylpyridine) were prepared as described previously.[27,35,36]

B. Physical Methods. The ^{1}H and ^{31}P NMR spectra were recorded at 293 K on a Bruker Avance 400 spectrometer. ^{1}H NMR chemical shifts were referenced to residual solvent as determined relative to Me_4Si (δ = 0 ppm). The ^{31}P{^{1}H} chemical shifts were reported in ppm relative to external 85% H_3PO_4. IR spectra were recorded on a Varian 800 FT-IR spectrometer. Elemental analyses were performed on a Carlo Erba EA 1110 CHN instrument at EPFL. X-ray diffraction studies were carried out in the EPFL Crystallographic Facility. Data collections were performed at low temperature using four-circle kappa diffractometers equipped with CCD detectors. Data were reduced and then corrected for absorption.[37] Solution, refinement, and geometrical calculations for all crystal structures were performed by SHELXTL.[38] Mössbauer spectra were recorded with a spectrometer from WissEL GmbH coupled to a closed-cycle cryostat from CRYO Industries of America Inc. The analysis of the spectra has been performed with the Software package Vinda assuming a Lorentzian line shape (http://whome.phys.au.dk/~hpg/vinda.htm). The spectra obtained at high fields were simulated using the spin-Hamiltonian formalism.[39]

C. Synthetic Methods. *Synthesis of [Fe(CO)$_2$(PPh$_3$)I(hp)] (Hhp =2-Hydroxy-pyridine) (**2**).* Na(hp) (137 mg, 1.17 mmol), prepared by mixing Hhp (111 mg, 1.17 mmol) and NaH (28 mg, 1.17 mmol) in tetrahydrofuran (THF), was added to a solution of $Fe(CO)_3(PPh_3)I_2$ (768 mg, 1.17 mmol) in ether (5 mL) under stirring conditions. After 1.5 h, the solvent was evaporated, and the solid residue was dissolved in a minimum quantity of CH_2Cl_2 and filtered. Pentane was added to the filtrate and a precipitate was formed. The precipitate was collected, washed with pentane, and dried under vacuum to afford **2** (560 mg, 0.94 mmol, 80%) as red crystals.

^{1}H NMR (400.13 MHz, $CDCl_3$): 7.86 (d, *J* = *5.2 Hz*, 1H), 7.52−7.29 (m, 15H), 7.06 (t, *J* = *7.6 Hz*, 1H), 6.35 (t, *J* = *6.0 Hz*, 1H), 5.55 ppm (d, *J* = *8.4 Hz*, 1H). ^{31}P NMR (162 MHz, $CDCl_3$): 73.3 ppm. IR (ν_{CO}, cm^{-1}): 2039 (s), 1988 (s). Anal. Calcd for $C_{25}H_{19}FeINO_3P$: C, 50.5; H, 3.2; N, 2.4. Found: C, 50.9; H, 3.2, N, 2.6.

*Synthesis of [Fe(CO)$_2$(PPh$_3$)I(hpp)] (Hhpp =2-Hydroxy-6-phenylpyridine) (**3**).* Using a similar procedure as described above, Na(hpp) (97 mg, 0.50 mmol), prepared by mixing Hhpp (86 mg, 0.50 mmol) and NaH (12 mg, 0.50 mmol) in THF, was added to a solution of $Fe(CO)_3(PPh_3)I_2$ (328 mg, 0.50 mmol) in ether (5 mL) under stirring conditions. After 0.5 h, the solvent was evaporated, and the solid residue was dissolved in a minimum quantity of CH_2Cl_2 and filtered. Pentane was added to the filtrate and a precipitate was formed. The precipitate was collected, washed with pentane, and dried under vacuum to afford **3** (280 mg, 0.42 mmol, 84%) as red crystals.

dx.doi.org/10.1021/ic200580z |*Inorg. Chem.* 2011, 50, 5249–5257

^{1}H NMR (400.13 MHz, $CDCl_3$): 7.94 (d, *J* = 7.2 *Hz*, 2H), 7.67 (t, *J* = 8.8 *Hz*, 2H), 7.52−7.22 (m, 16H), 7.09 (t, *J* = 8.0 Hz, 1H), 6.37 (d, *J* = 8.0 Hz, 1H), 5.59 ppm (d, *J* = 8.0 Hz, 1H). ^{31}P NMR (162 MHz, $CDCl_3$): 71.2 ppm. IR (ν_{CO}, cm^{-1}): 2035 (s), 2001 (s). Anal. Calcd for $C_{31}H_{23}FeINO_3P$: C, 55.5; H, 3.5; N, 2.1. Found: C, 54.8; H, 3.5, N, 2.6.

Synthesis of [Fe(CO)$_2$(PEt$_3$)I(hmp)] (***4***). Using a similar procedure as described above, Na(hmp) (87 mg, 0.67 mmol), prepared by mixing Hhmp (73 mg, 0.67 mmol) and NaH (16 mg, 0.67 mmol) in THF, was added to a solution of $Fe(CO)_3(PEt_3)I_2$ (341 mg, 0.67 mmol) in ether (5 mL) under stirring conditions. After 3.0 h, the solvent was evaporated, and the solid residue was dissolved in a minimum quantity of CH_2Cl_2 and filtered. Pentane was added to the filtrate, and a precipitate was formed. The precipitate was collected, washed with pentane, and dried under vacuum to afford **4** (200 mg, 0.43 mmol, 64%) as red crystals.

^{1}H NMR (400.13 MHz, $CDCl_3$): 7.35 (t, *J* = 8.0 Hz, 1H), 6.36 (d, *J* = 8.0 Hz, 1H), 5.89 (d, *J* = 8.0 Hz, 1H), 2.47 (s, 3H), 1.75 (m, 6H), 1.15 ppm (m, 9H). ^{31}P NMR (162 MHz, $CDCl_3$): 70.0 ppm. IR (ν_{CO}, cm^{-1}): 2026 (s), 1974 (s). Anal. Calcd for $C_{14}H_{21}FeINO_3P$: C, 36.2; H, 4.6; N, 3.0. Found: C, 36.2; H, 4.6, N, 3.1.

Synthesis of [Fe(CO)$_2$(PPh$_3$)(hmp){S(2-iPr−C$_6$H$_4$)}] (***6***). NaS(2-*i*Pr−C_6H_4) (101 mg, 0.58 mmol), prepared by mixing HS(2-*i*Pr−C_6H_4) (88 mg, 0.58 mmol) and NaH (14 mg, 0.58 mmol) in ether, was added to a solution of [Fe(CO)$_2$(PPh$_3$)I(hmp)] (**1**) (353 mg, 0.58 mmol) in CH_2Cl_2 (5 mL) under stirring conditions. The resulting solution was stirred for 1.5 h and then the precipitate was filtered off. The filtrate was evaporated in vacuum, and the solid residue was recrystallized from dichlomethane/pentane at −30 °C to afford **6**·CH_2Cl_2 (100 mg, 0.14 mmol, 24%) as red crystals.

^{1}H NMR (400.13 MHz, $CDCl_3$): 7.66 (d, *J* = 8.0 Hz, 1H), 7.52−7.26 (m, 15H), 7.16−7.09 (m, 2H), 6.92−6.85 (m, 2H), 6.05 (d, *J* = 8.0 Hz, 1H), 5.34 (d, *J* = 8.0 Hz, 1H), 5.30 (s, 2H, CH_2Cl_2), 4.10 (m, 1H), 2.21 (s, 3H), 1.21 ppm (dd, J_1 = 8.0 Hz, J_2 = 2.4 Hz, 6H). ^{31}P NMR (162 MHz, $CDCl_3$): 54.0 ppm. IR (ν_{CO}, cm^{-1}): 2025 (s), 1985 (s). Anal. Calcd for $C_{36}H_{34}Cl_2FeNO_3PS$: C, 60.2; H, 4.8; N, 2.0. Found: C, 60.0; H, 4.8, N, 2.2.

Synthesis of [Fe(CO)$_2$(PPh$_3$)(hmp){S(2,4,6-Me$_3$C$_6$H$_2$)}] (***7***). Using a similar procedure as described above. NaS(2,4,6-$Me_3C_6H_2$) (204 mg, 1.17 mmol), prepared by mixing HS(2,4,6-$Me_3C_6H_2$) (178 mg, 1.17 mmol) and NaH (28 mg, 1.17 mmol) in ether, was added to a solution of [Fe(CO)$_2$(PPh$_3$)I(hmp)] (**1**) (712 mg, 1.17 mmol) in CH_2Cl_2 (5 mL) under stirring conditions. The resulting solution was stirred for 15 min and then the precipitate was filtered off. The filtrate was evaporated in vacuum, and the solid residue was recrystallized from dichlomethane/pentane at −30 °C to afford **7** (350 mg, 0.55 mmol, 47%) as red crystals.

^{1}H NMR (400.13 MHz, $CDCl_3$): 7.40−7.25 (m, 15H), 6.87 (t, *J* = 8.0 Hz, 1H), 6.82 (s, 2H), 6.07 (d, *J* = 8.0 Hz, 1H), 5.25 (d, *J* = 8.0 Hz, 1H), 2.55 (s, 6H), 2.31 (s, 3H), 2.17 ppm (s, 3H). ^{31}P NMR (162 MHz, $CDCl_3$): 53.3 ppm. IR (ν_{CO}, cm^{-1}): 2021 (s), 1973 (s). Anal. Calcd for $C_{35}H_{32}FeNO_3PS$: C, 66.4; H, 5.1; N, 2.2. Found: C, 65.9; H, 5.1, N, 2.3.

Synthesis of [Fe(CO)$_2$(PPh$_3$)I{S(C$_5$H$_4$N)}] (***8***). NaS(C_5H_4N) (156 mg, 1.17 mmol), prepared by mixing HS(C_5H_4N) (130 mg, 1.17 mmol) and NaH (28.1 mg, 1.17 mmol) in THF, was added to a solution of [Fe(CO)$_2$(PPh$_3$)I$_2$] (770 mg, 1.17 mmol) in ether (10 mL) under stirring in dark. After 1 h, the solvent was evaporated, and the solid residue was dissolved in a minimum quantity of CH_2Cl_2 and filtered. Ether was added to the filtrate, and a precipitate was formed. The precipitate was collected and recrystallized from dichlomethane/ether at −30 °C to afford **8** (430 mg, 0.74 mmol, 60%) as red crystals.

^{1}H NMR (400.13 MHz, CD_3CN): 8.05 (d, *J* = 4.0 Hz, 1H), 7.60−7.20 (m, 15H), 7.10 (t, *J* = 8.0 Hz, 1H), 6.67 (d, *J* = 6.0 Hz, 1H), 6.14 ppm (d, *J* = 8.0 Hz, 1H). ^{31}P NMR (162 MHz, CD_3CN): 75.8 ppm. IR (ν_{CO}, cm^{-1}): 2028 (s), 1986 (s). Anal. Calcd for $C_{25}H_{19}FeINO_2PS$: C, 49.1; H, 3.1; N, 2.3. Found: C, 49.4; H, 3.1, N, 2.3.

Synthesis of [Fe(CO)$_2$(PPh$_3$)I{S(6-Me-C$_5$H$_3$N)}] (***9***). NaS(6-Me-C_5H_3N) (130 mg, 0.89 mmol), prepared by mixing HS(6-Me-C_5H_3N) (111 mg, 0.89 mmol) and NaH (21.4 mg, 0.89 mmol) in THF, was added to a solution of [Fe(CO)$_2$(PPh$_3$)I$_2$] (585 mg, 0.89 mmol) in ether (10 mL) under stirring in the dark. After 0.5 h, the solvent was evaporated, and the solid residue was dissolved with a minimum quantity of CH_2Cl_2 and filtered. Ether was added to the filtrate, and a precipitate was formed. The precipitate was collected and recrystallized from dichlomethane/ether at −30 °C to afford **9** (350 mg, 0.56 mmol, 63%) as red crystals.

^{1}H NMR (400.13 MHz, $CDCl_3$): 7.50−7.22 (m, 15H), 6.98 (t, *J* = 8.0 Hz, 1H), 6.52 (d, *J* = 8.0 Hz, 1H), 5.97 (d, *J* = 8.0 Hz, 1H), 2.37 ppm (s, 3H). ^{31}P NMR (162 MHz, $CDCl_3$): 73.2 ppm. IR (ν_{CO}, cm^{-1}): 2018 (s), 1968 (s). Anal. Calcd for $C_{26}H_{21}FeINO_2PS$: C, 50.0; H, 3.4; N, 2.2. Found: C, 50.1; H, 3.2, N, 1.9.

*Synthesis of cis-(I, PPh$_3$)-Fe(CO)$_2$(PPh$_3$)I(OMe-PyS) (**10a**) and trans-(I, PPh$_3$)-Fe(CO)$_2$(PPh$_3$)I(OMe-PyS) (**10b**).* NaS(6-OMe-C_5H_3N) (76.1 mg, 0.47 mmol), prepared by mixing HS(6-OMe-C_5H_3N) (65.5 mg, 0.47 mmol) and NaH (11.2 mg, 0.47 mmol) in THF, was added to a solution of [Fe(CO)$_2$(PPh$_3$)I$_2$] (305 mg, 0.47 mmol) in ether (10 mL) under stirring in the dark. After 0.5 h, the solvent was evaporated, and the solid residue was dissolved with a minimum quantity of CH_2Cl_2 and filtered. Ether was added to the filtrate, and a precipitate formed. The precipitate was collected to afford **10a** (160 mg, 0.25 mmol, 53%) as an orange powder. Leaving the solution of **10a** in CH_2Cl_2 overnight in the dark afforded **10b** quantitatively, which was isolated as a red powder after evaporation.

10a: ^{1}H NMR (400.13 MHz, $CDCl_3$): 7.80−7.38 (m, 16H), 6.44 (d, *J* = 8.0 Hz, 1H), 6.33 (d, *J* = 8.0 Hz, 1H), 3.91 ppm (s, 3H). ^{31}P NMR (162 MHz, $CDCl_3$): 51.1 ppm. IR (ν_{CO}, cm^{-1}): 2031 (s), 1980 (s). Anal. Calcd for $C_{26}H_{21}FeINO_3PS$: C, 48.7; H, 3.3; N, 2.2. Found: C, 49.0; H, 3.8, N, 2.1.

10b: ^{1}H NMR (400.13 MHz, $CDCl_3$): 7.57−7.23 (m, 15H), 7.11 (t, *J* = 8.0 Hz, 1H), 6.04 (d, *J* = 8.0 Hz, 1H), 5.86 (d, *J* = 8.0 Hz, 1H), 3.84 ppm (s, 3H). ^{31}P NMR (162 MHz, $CDCl_3$): 75.3 ppm. IR (ν_{CO}, cm^{-1}): 2024 (s), 1977 (s). Anal. Calcd for $C_{26}H_{21}FeINO_3PS$: C, 48.7; H, 3.3; N, 2.2. Found: C, 48.4; H, 3.4, N, 2.0.

*Synthesis of [Fe(CO)$_2$(PPh$_3$)$_2${S(6-Me-C$_5$H$_3$N)}]$^+$(PF$_6$)$^-$ (**11**).* $TlPF_6$ (91 mg, 0.26 mmol) and PPh_3 (68 mg, 0.26 mmol) were added into a solution of [Fe(CO)$_2$(PPh$_3$)I{S(6-Me-C_5H_3N)}] (**9**) (81 mg, 0.13 mmol) in CH_3CN (5 mL) under stirring. After 4.5 h, the solvent was evaporated, and the solid residue was dissolved in a minimum quantity of CH_2Cl_2 and filtered. Pentane was added to the filtrate, and a precipitate was formed. The precipitate was collected and recrystallized from dichlomethane/pentane at −30 °C to afford **11** (78 mg, 0.086 mmol, 66%) as red crystals.

^{1}H NMR (400.13 MHz, $CDCl_3$): 7.81−7.32 (m, 30H), 6.65 (t, *J* = 7.2 Hz, 1H), 6.49 (d, *J* = 7.2 Hz, 1H), 5.29 (d, *J* = 7.2 Hz, 1H), 2.09 ppm (s, 3H). ^{31}P NMR (162 MHz, $CDCl_3$): 49.6, −143.2 ppm. IR (ν_{CO}, cm^{-1}): 2025 (s), 1989 (s). Anal. Calcd for $C_{44}H_{36}F_6FeNO_2P_3S$·$0.2CH_2Cl_2$: C, 57.5; H, 4.0; N, 1.5. Found: C, 57.2; H, 4.0, N, 1.7.

Synthesis of [Fe(CO)$_2$I(2,6-Me$_2$C$_6$H$_3$NC)(SC$_5$H$_4$N-CO)] (***13***). NaS-(C_5H_4N) (93 mg, 0.70 mmol), prepared by mixing HSC_5H_4N (77 mg, 0.70 mmol) and NaH (16.6 mg, 0.70 mmol) in THF, was added to a solution of $Fe(CO)_3(2,6\text{-}Me_2C_6H_3NC)I_2$ (364 mg, 0.70 mmol) in ether (5 mL) under stirring. After 0.5 h, the solvent was evaporated, and the solid residue was dissolved in a minimum quantity of CH_2Cl_2 and filtered. Pentane was added to the filtrate, and a precipitate was formed. The precipitate was collected and recrystallized from dichlomethane/pentane at −30 °C to afford **13** (90 mg, 0.18 mmol, 25%) as orange crystals. When the reaction was carried out under CO (1 atm), the yield increased to 42%.

^{1}H NMR (400.13 MHz, $CDCl_3$): 8.42 (br s, 1H), 7.79 (d, *J* = 8.0 Hz, 1H), 7.58 (t, *J* = 8.0 Hz, 1H), 7.18 (d, *J* = 8.0 Hz, 1H), 7.10−7.00

(m, 3H), 2.38 ppm (s, 6H). IR ($\nu_{CO/NC}$, cm^{-1}): 2177 (m, *NC*), 2041 (s, terminal *CO*), 2007 (s, terminal *CO*) 1700 (s, acyl *CO*). Anal. Calcd for $C_{17}H_{13}FeIN_2O_3S$: C, 40.2; H, 2.6; N, 5.5. Found: C, 40.0; H, 2.6, N, 5.4.

■ ASSOCIATED CONTENT

Supporting Information. Crystallographic details, structural drawing of complexes **2**, **4**, **6**, **10a**, **10b**, **11**, Mössbauer spectra of **5**, **9**, **13**, **17**. This material is available free of charge via the Internet at http://pubs.acs.org.

■ AUTHOR INFORMATION

Corresponding Author
*E-mail: xile.hu@epfl.ch.

■ ACKNOWLEDGMENT

The work at EPFL is supported by the Swiss National Science Foundation (project no. 200021_119663). V.S. acknowledges the support of NANOKAT.

■ REFERENCES

(1) Vignais, P. M.; Billoud, B.; Meyer, J. *FEMS Microbiol. Rev.* **2001**, *25*, 455–501.
(2) Shima, S.; Thauer, R. K. *Chem. Rec.* **2007**, *7*, 37–46.
(3) Tard, C.; Pickett, C. J. *Chem. Rev.* **2009**, *109*, 2245–2274.
(4) Thauer, R. K.; Klein, A. R.; Hartmann, G. C. *Chem. Rev.* **1996**, *96*, 3031–3042.
(5) Volbeda, A.; Charon, M. H.; Piras, C.; Hatchikian, E. C.; Frey, M.; Fontecilla-Camps, J. C. *Nature* **1995**, *373*, 580–587.
(6) Nicolet, Y.; Piras, C.; Legrand, P.; Hatchikian, C. E.; Fontecilla-Camps, J. C. *Struct. Fold. Des.* **1999**, *7*, 13–23.
(7) Peters, J. W.; Lanzilotta, W. N.; Lemon, B. J.; Seefeldt, L. C. *Science* **1998**, *282*, 1853–1858.
(8) Armstrong, F. A. *Curr. Opin. Chem. Biol.* **2004**, *8*, 133–140.
(9) Vincent, K. A.; Parkin, A.; Armstrong, F. A. *Chem. Rev.* **2007**, *107*, 4366–4413.
(10) Shima, S.; Lyon, E. J.; Sordel-Klippert, M. S.; Kauss, M.; Kahnt, J.; Thauer, R. K.; Steinbach, K.; Xie, X. L.; Verdier, L.; Griesinger, C. *Angew. Chem., Int. Ed.* **2004**, *43*, 2547–2551.
(11) Lyon, E. J.; Shima, S.; Boecher, R.; Thauer, R. K.; Grevels, F. W.; Bill, E.; Roseboom, W.; Albracht, S. P. J. *J. Am. Chem. Soc.* **2004**, *126*, 14239–14248.
(12) Shima, S.; Lyon, E. J.; Thauer, R. K.; Mienert, B.; Bill, E. *J. Am. Chem. Soc.* **2005**, *127*, 10430–10435.
(13) Korbas, M.; Vogt, S.; Meyer-Klaucke, W.; Bill, E.; Lyon, E. J.; Thauer, R. K.; Shima, S. *J. Biol. Chem.* **2006**, *281*, 30804–30813.
(14) Shima, S.; Pilak, O.; Vogt, S.; Schick, M.; Stagni, M. S.; Meyer-Klaucke, W.; Warkentin, E.; Thauer, R. K.; Ermler, U. *Science* **2008**, *321*, 572–575.
(15) Hiromoto, T.; Ataka, K.; Pilak, O.; Vogt, S.; Stagni, M. S.; Meyer-Klaucke, W.; Warkentin, E.; Thauer, R. K.; Shima, S.; Ermler, U. *FEBS Lett.* **2009**, *583*, 585–590.
(16) Hiromoto, T.; Warkentin, E.; Moll, J.; Ermler, U.; Shima, S. *Angew. Chem., Int. Ed.* **2009**, *48*, 6457–6460.
(17) Salomone-Stagni, M.; Stellato, F.; Whaley, C. M.; Vogt, S.; Morante, S.; Shima, S.; Rauchfuss, T. B.; Meyer-Klaucke, W. *Dalton Trans.* **2010**, *39*, 3057–3064.
(18) Shima, S.; Vogt, S.; Göbels, A.; Bill, E. *Angew. Chem., Int. Ed.* **2010**, *49*, 9917–9921.
(19) Guo, Y. S.; Wang, H. X.; Xiao, Y. M.; Vogt, S.; Thauer, R. K.; Shima, S.; Volkers, P. I.; Rauchfuss, T. B.; Pelmenschikov, V.; Case, D. A.; Alp, E. E.; Sturhahn, W.; Yoda, Y.; Cramer, S. P. *Inorg. Chem.* **2008**, *47*, 3969–3977.
(20) Wright, J. A.; Turrell, P. J.; Pickett, C. J. *Organometallics* **2010**, *29*, 6146–6156.
(21) Wang, X. F.; Li, Z. M.; Zeng, X. R.; Luo, Q. Y.; Evans, D. J.; Pickett, C. J.; Liu, X. M. *Chem. Commun.* **2008**, 3555–3557.
(22) Turrell, P. J.; Wright, J. A.; Peck, J. N. T.; Oganesyan, V. S.; Pickett, C. J. *Angew. Chem., Int. Ed.* **2010**, *49*, 7508–7511.
(23) Li, B.; Liu, T.; Popescu, C. V.; Bilko, A.; Darensbourg, M. Y. *Inorg. Chem.* **2009**, *48*, 11283–11289.
(24) Liu, T. B.; Li, B.; Popescu, C. V.; Bilko, A.; Perez, L. M.; Hall, M. B.; Darensbourg, M. Y. *Chem.—Eur. J.* **2010**, *16*, 3083–3089.
(25) Royer, A. M.; Rauchfuss, T. B.; Gray, D. L. *Organometallics* **2009**, *28*, 3618–3620.
(26) Royer, A. M.; Salomone-Stagni, M.; Rauchfuss, T. B.; Meyer-Klaucke, W. *J. Am. Chem. Soc.* **2010**, *132*, 16997–17003.
(27) Obrist, B. V.; Chen, D. F.; Ahrens, A.; Schunemann, V.; Scopelliti, R.; Hu, X. L. *Inorg. Chem.* **2009**, *48*, 3514–3516.
(28) Chen, D. F.; Scopelliti, R.; Hu, X. L. *J. Am. Chem. Soc.* **2010**, *132*, 928–929.
(29) Chen, D. F.; Scopelliti, R.; Hu, X. L. *Angew. Chem., Int. Ed.* **2010**, *49*, 7512–7515.
(30) Tanino, S.; Ohki, Y.; Tatsumi, K. *Chem. Asian. J.* **2010**, *5*, 1962–1964.
(31) See Supporting Information.
(32) Schunemann, V.; Paulsen, H. In *Application of Physical Methods to Inorganic and Bioinorganic Chemistry*; Scott, R. A., Lukehart, C. M., Eds.; John Wiley & Sons Ltd.: New York, 2007; pp 243−269.
(33) Gütlich, P.; Ensling, J. In *Inorganic electronic structure and spectroscopy*; Solomon, E. I., Lever, A. B. P., Eds.; Wiley-Interscience: Hoboken, NJ, 2006; Vol. 1, pp 161−211.
(34) Gütlich, P.; Ensling, J. In *Inorganic Electronic Structure and Spectroscopy*; Solomon, E. I., Lever, A. B. P., Eds.; John Wiley & Sons, Inc.: Hoboken, NJ, 1999; Vol. 1, p 161.
(35) Bellachioma, G.; Cardaci, G.; Macchioni, A.; Venturi, C.; Zuccaccia, C. *J. Organomet. Chem.* **2006**, *691*, 3881–3888.
(36) Taylor, R. C.; Horrocks, W. D. *Inorg. Chem.* **1964**, *3*, 584–589.
(37) Blessing, R. H. *Acta Crystallogr., Sect. A* **1995**, *51*, 33–38.
(38) Sheldrick, G. M. *SHELXTL*, release 6.1.4; Bruker AXS Inc.: Madison, WI, 2003.
(39) Trautwein, A. X.; Bominaar, E. L.; Winkler, H. In *Structure and Bonding: Bioinorganic Chemistry*; Clarke, M. J., Goodenough, J. B., Ibers, J. A., Jørgensen, C. K., Mingos, D. M. P., Neilands, J. B., Palmer, G. A., Reinen, D., Sadler, P. J., Weiss, R., Williams, R. J. P., Eds.; Springer: Berlin, 1991; Vol. 78, pp 1−95.